Available online at www.sciencedirect.com
ScienceDirect
ELSEVIER
Journal of Sound and Vibration 308 (2007) 44–66
JOURNAL OF SOUND AND VIBRATION
www.elsevier.com/locate/jsvi

Statistical moments predictions for a moored floating body oscillating in random waves

Antonio Culla*, Antonio Carcaterra

Department of Mechanics and Aeronautics, University of Rome, "La Sapienza", Via Eudossiana, 18, 00184 Roma, Italy

Received 18 July 2006; received in revised form 4 July 2007; accepted 4 July 2007

Abstract

Two statistical techniques are developed to predict the statistical moments of the horizontal motion of a floating moored dock, known as catenary anchor leg mooring (CALM), loaded by hydrodynamic random forces. The dock is represented by a lumped mass, the mooring cables by equivalent nonlinear springs and the hydrodynamic forces are modelled by a modified Morison equation. The model of the floating dock leads to a nonlinear ordinary differential equation. Although the problem could be approached by a direct numerical integration, e.g. by Monte-Carlo simulations, because of the stochastic nature of the excitation, this would imply a large number of runs to produce results of some statistical significance. In the present paper an alternative solution is based on the development of two more efficient techniques to predict the relevant statistical moments of the dock response.

The first method, called CPSP (conventional perturbation–statistical perturbation), is based on the application of two subsequent perturbation techniques, the first relying on a classical perturbation method, the second on a statistical perturbation approach.

The second method, called SLSP (statistical linearization–statistical perturbation), combines indeed a statistical linearization approach together with a statistical perturbation approach.

The procedures allow the linearization of the cables restoring forces as well as of the hydrodynamic load and they can be easily generalized to be applied to different dock configurations or to systems of different physical nature. The results, compared with those obtained by a Monte-Carlo simulations, show, in terms of statistical moments of the dock response, a satisfactory agreement.

1. Introduction

The physical system analysed represents a prototype model for those structures called catenary anchor leg mooring frequently used in marine and offshore engineering [1–4]. A buoying system, restrained by a set of cables anchored to the sea bottom, is forced by random incoming waves [5–7]. The focus in the prediction of some statistics of the buoying system response to wave loads [8,9]. In the model considered in the present paper, the random wave load does not appear in the equation of the motion only as a known forcing term, but

*Corresponding author. Tel.: +39 0644585556; fax: +39 06484854.
E-mail address: antonio.culla@uniroma1.it (A. Culla).

0022-460X/$ - see front matter
doi:10.1016/j.jsv.2007.07.018

it affects the system dynamics by the presence of random coefficients appearing in the nonlinear equation of the motion.

The mathematical tool to deal with this physical system belongs to a class of methods only recently considered in the technical literature. In fact, while the case in which a deterministic dynamic system is forced by random loads is a well-established problem in the context of random oscillations [10–12], the case in which the system is indeed itself random due to its interaction with external random forces is more complicated. Examples of these problems have been recently considered in engineering, especially in the context for which a fluid–structure interaction is involved [13–17]. Although Monte-Carlo simulations can provide meaningful statistics for these systems, this implies time-consuming numerical computations. Alternatively, more smart approaches can be developed in order to predict some statistical moments of the solution (often that of second order) through appropriate techniques, as those proposed in this paper, the classical perturbation–stochastic perturbation (CPSP) and the statistical linearization–stochastic perturbation (SLSP) [12,18–21].

In Section 2 a model for the cable restoring forces is presented based on the static force–displacement relationship (Section 2.1) and on a suitable reduction to a cubic nonlinearity (Section 2.2).

Section 3 describes the model used to represent the random hydrodynamic load on the buoying system. The results of Sections 2 and 3 are combined together in Section 4 to derive a prototype equation for the investigated system.

In Section 5 the mathematical nature of the problem is clarified to justify the development of the two solution techniques proposed, namely the CPSP and the SLSP, illustrated in details in Sections 6 and 7, respectively.

Finally in Section 8 several numerical simulations are presented comparing the performances of the two techniques and their predictions, in terms of statistical moments, with those obtained by a direct integration of the equation of motion.

2. Nonlinear cable model

The nonlinear equations of a uniform inextensible cable suspended among two fixed points are considered. The cable can support only tensile static forces in absence of any flexural rigidity. In Section 2.1 the nonlinear force–displacement relationship for a single cable with one end attached to the sea bottom and the other to the buoying system is determined. In Section 2.2 a pair of cables, symmetrically attached to the same structure, is considered, simplifying the force–displacement relationship for the restoring force by a cubic nonlinearity.

2.1. Nonlinear statics of the cable

Some results from the theory of cables form the basis for reducing the restoring forces to a cubic nonlinearity as illustrated in Section 2.2.

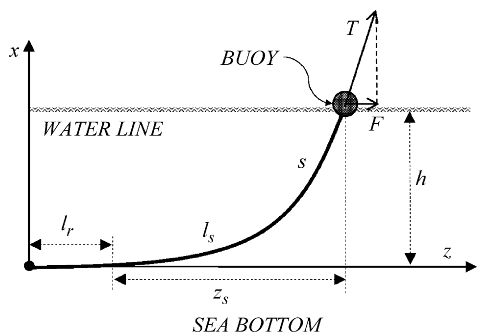

Fig. 1. Cable configuration and characteristic parameters.

Let s be the curvilinear abscissa, x and z Cartesian coordinates of the cable points (see Fig. 1), T the tension along the cable and W its weight per unit length. The static equations of the cable read [5]:

$$\begin{cases} \dfrac{\partial}{\partial s}\left(T\dfrac{\partial x}{\partial s}\right) = W, \\ \dfrac{\partial}{\partial s}\left(T\dfrac{\partial z}{\partial s}\right) = 0. \end{cases} \tag{1}$$

Integration of the second equation of (1), produces

$$T\frac{\partial z}{\partial s} = F, \tag{2}$$

where F is the horizontal component of T, constant when loads along z are absent.

Inextensibility along the axial direction implies

$$\left(\frac{\partial x}{\partial s}\right)^2 + \left(\frac{\partial z}{\partial s}\right)^2 = 1. \tag{3}$$

Substitution of (2) and (3) in (1) produces an equation for which the analytical solution is found:

$$x(z) = \frac{F}{W}\cosh\left(\frac{Wz}{F} + \frac{W}{F}c_1\right) + c_2. \tag{4}$$

The constants c_1 and c_2 are determined by the boundary conditions. Assuming the cable configuration as shown in Fig. 1, boundary conditions are:

$$\begin{cases} \left.\dfrac{\partial x}{\partial s}\right|_0 = 0, \\ x|_0 = 0. \end{cases} \tag{5}$$

Thus

$$x(z) = \frac{F}{W}\left[\cosh\left(\frac{Wz}{F}\right) - 1\right] \quad z(x) = \frac{F}{W}\sinh^{-1}\left[\sqrt{\left(\frac{Wx}{F}\right)^2 + 2\frac{Wx}{F}}\right]. \tag{6}$$

Eq. (6) provides the force–displacement relationship at each cable point.

The suspended length l_s of the cable—depending on z—follows from Eqs. (3) and (6) as

$$s(z) = \int_0^z \sqrt{1 + \left(\frac{\partial x}{\partial z}\right)^2}\,\mathrm{d}z \to l_s(z) = \frac{F}{W}\sinh\left(\frac{Wz}{F}\right) \tag{7}$$

and combining the two previous equations:

$$l_s(x) = x\sqrt{\frac{2F}{Wx} + 1}. \tag{8}$$

This expression permits to estimate the minimum cable length required for safety reasons. In fact, known $F_{\max}$, i.e. the maximum expected F for the worst operating condition, the minimum cable length follows:

$$l_{s\,\min} = h\sqrt{\frac{2F_{\max}}{Wh} + 1}, \tag{9}$$

where h is the sea depth. For $F = F_{\max}$, the whole cable is suspended and $l_{s\,\min}$ is the minimum length that still warrants a zero slope of the cable line at the anchor point on the sea bottom. This implies the absence of vertical forces on the anchor, satisfying an important safety requirement.

During the normal operation service $F < F_{\max}$ and the length l_r of the cable lies on the bottom (see Fig. 1); z_s is the length of the projection on the horizontal abscissa of the suspended part of the cable. The horizontal distance between the anchor (bottom end) and the fairlead of the mooring line (cable end at the water line) is given by the following equation:

$$d_c = l_r + z_s, \tag{10}$$

where l_r is determined from the difference between $l_{s\,\min}$ and l_s, z_s from Eq. (7) for $x(z_s) = h$. Thus,

$$d_c = h\sqrt{2\frac{F_{\max}}{Wh}+1} - h\sqrt{2\frac{F}{Wh}+1} + \frac{F}{W}\cosh^{-1}\left(1+\frac{Wh}{F}\right). \tag{11}$$

This provides the constitutive nonlinear force–distance relationship for the cable.

2.2. Reduction to a cubic nonlinearity

The mooring actions on the dock can be approximated by a simpler cubic restoring force. In offshore structures, often, pairs of cables are anchored to the seabed acting in opposite directions, as shown in Fig. 3.

In this configuration the total restoring force of the pair of cables is given by

$$F_T(w_c) = F(d_c^{\text{left}}) - F(d_c^{\text{right}}) = F_+ - F_-, \tag{12}$$

where $d_c^{\text{left}} = w_{c0} + w_c$, $d_c^{\text{right}} = w_{c0} - w_c$ and w_{c0} is the horizontal distance between the anchor and the fairlead of the mooring line for both the cables in the static reference configuration, while w_c is the horizontal end displacement of the cables (Fig. 2).

A Taylor series expansion of F_T up to the third-order provides

$$F_T(w_c) = F_T|_0 + \left.\frac{\partial F_T}{\partial w_c}\right|_0 w_c + \frac{1}{2}\left.\frac{\partial^2 F_T}{\partial w_c^2}\right|_0 w_c^2 + \frac{1}{6}\left.\frac{\partial^3 F_T}{\partial w_c^3}\right|_0 w_c^3, \tag{13}$$

where the derivatives are calculated at $w_c = 0$ or $d_c = w_{c0}$.

This equation involves the derivatives of $F_T(w_c)$, while the force–displacement relationship is available through the inverse displacement–force dependency $w_c(F_T)$. However, because of the equation:

$$\frac{\partial w_c}{\partial F}\frac{\partial F}{\partial w_c} = 1 \tag{14}$$

the first derivative of $F_T(w_c)$ is obtained in terms of the first derivative of $w_c(F_T)$. Using an analogous idea, higher order derivatives are obtained recursively:

$$\begin{aligned}
&\frac{\partial^{(i)}}{\partial F^i}\left(\frac{\partial w_c}{\partial F}\frac{\partial F}{\partial w_c}\right) = 0,\\
&\frac{\partial}{\partial F}\left(\frac{\partial^{(i)} F}{\partial w_c^i}\right) = \frac{\partial^{(i+1)} F}{\partial w_c^{i+1}}\frac{\partial w_c}{\partial F},\\
&\partial F_\pm/\partial w_c = \pm\partial F/\partial w_c
\end{aligned} \tag{15}$$

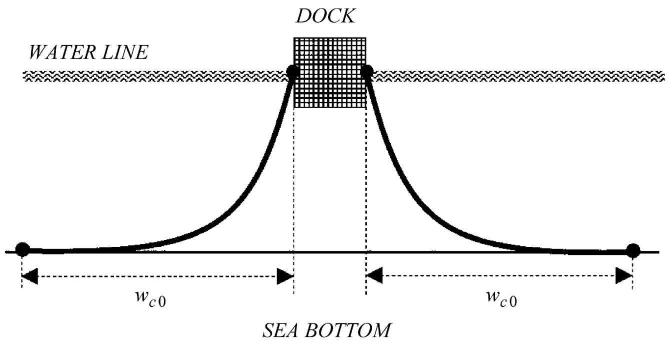

Fig. 2. Moored dock configuration.

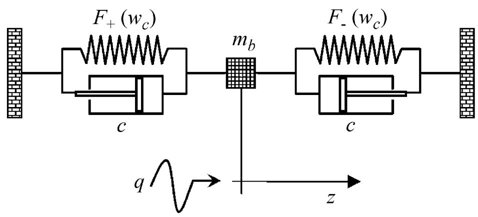

Fig. 3. Equivalent 1DOF model.

and explicitly up to the third order:

$$\frac{\partial F}{\partial w_c}=\frac{1}{\partial w_c/\partial F},\quad \frac{\partial^2 F}{\partial w_c^2}=-\frac{\partial^2 w_c/\partial F^2}{(\partial w_c/\partial F)^3},\quad \frac{\partial^3 F}{\partial w_c^3}=-\frac{3(\partial^2 w_c/\partial F^2)^2-(\partial^3 w_c/\partial F^3)(\partial w_c/\partial F)}{(\partial w_c/\partial F)^5}. \tag{16}$$

This implies:

$$F_T(w_c)=\gamma_1 w_c+\gamma_3 w_c^3 \tag{17}$$

and

$$\gamma_1=\left.\frac{2}{\partial w_c/\partial F}\right|_{F_0},\quad \gamma_3=-\left.\frac{3\left(\dfrac{\partial^2 w_c}{\partial F^2}\Big/\dfrac{\partial w_c}{\partial F}\right)^2-\dfrac{\partial^3 w_c}{\partial F^3}\Big/\dfrac{\partial w_c}{\partial F}}{3\left(\dfrac{\partial w_c}{\partial F}\right)^3}\right|_{F_0} \tag{18}$$

the terms of order zero and two are void and, under the hypothesis of small displacements, a cubic dependence of the horizontal force on the displacement of the cable end is determined (Fig. 3).

3. Random hydrodynamic load

The modified Morison equation [4,6–9] provides the wave load q per unit length on a circular cylinder in terms of the fluid–structure relative velocity $(\dot{\xi}-\dot{w})$:

$$q(t)=C_I\ddot{\xi}+m_a\ddot{w}+C_D|\dot{\xi}-\dot{w}|(\dot{\xi}-\dot{w}), \tag{19}$$

where $w=w_c$, $\xi(x,z,t)$ is the horizontal fluid particle displacement, assumed approximately the same for each point of the wetted surface of the dock, C_I and C_D are the inertia and the drag coefficient, respectively, and m_a is the added mass. These coefficients depend on the dimension of the dock, the water density and some non-dimensional quantity. Namely:

$$C_I=(1+c_a)\frac{\rho_w\pi D^2}{4},\quad C_D=\frac{1}{2}c_d\rho_w D,\quad m_a=c_a\frac{\rho_w\pi D^2}{4}, \tag{20}$$

where c_a is the non-dimensional added mass coefficient ($c_a\cong 1$), ρ_w is the seawater density, D is the dock diameter and c_d is the non-dimensional drag coefficient ($0.6\leqslant c_d\leqslant 1.2$).

ξ represents a random process, and Eq. (19) represents a hydrodynamic random load. There are different possibilities to characterize the random nature of $\xi(x,z,t)$. The first is to assume it as a (Gaussian) white noise.

A more refined approach uses indeed some information on the fluid motion generated by surface waves. The Airy theory provides

$$\xi(x,t)=\sum_{n=-\infty}^{\infty}B_n(\omega_n,\varphi_n,x)\chi_n(t), \tag{21}$$

where

$$B_n=\tfrac{1}{2}A_n(\sin\varphi_n+j\cos\varphi_n),\quad B_{-n}=B_n^*,\quad \chi_n(t)=e^{j\omega_n t} \tag{22}$$

are statistically independent random complex coefficients, i.e.

$$E\{B_n B_m^*\} = \begin{cases} 0 & \text{for } n \neq m, n > 0, m > 0, \\ E\{B_n B_n^*\} = \sigma_{B_n}^2 & \text{for } n = m, \end{cases}$$

where ω_n is the wave frequency, g the gravity acceleration and φ_n a random phase (e.g. uniformly distributed over the interval [0, 2π]). The amplitude coefficients, A_n, are given by

$$A_n(\omega_n, x) = \sqrt{2S(\omega_n)\frac{\omega_n}{n}}\frac{\cosh\left((\omega_n^2/g)x\right)}{\sinh\left((\omega_n^2/g)h\right)}, \tag{23}$$

where h is the sea depth and $S(\omega_n)$ is the nth spectral component of the Pierson–Moskowitz spectrum [5]:

$$S(\omega_n) = \frac{\alpha g^2}{\omega_n^5}\mathrm{e}^{-\beta\left(g/(U\omega_n)\right)^4} \tag{24}$$

with U the wind velocity, α and β are non-dimensional parameters—often $\alpha = 8.1 \times 10^{-3}$ and $\beta = 0.74$.

4. The floating dock with mooring lines

The present model of the floating dock introduces several approximations: (i) the dock is considered a point of mass m_b, (ii) the pair of cables is approximated by two nonlinear cubic springs, (iii) the hydrodynamic force is determined by the Morison equation and (iv) energy dissipation is introduced by a viscous damping (of characteristic constant $\tilde{c}$). With these assumptions, the equation of the dock motion is

$$m_b\ddot{w} + 2\tilde{c}\dot{w} + F_T(w_c) = q(t), \tag{25}$$

where $w = w_c$ is the dock center of mass displacement. Explicit form for the forces F_T and q produces

$$(m_b - m_a)\ddot{w} + 2\tilde{c}\dot{w} + \gamma_1 w + \left[-C_D|\dot{\xi} - \dot{w}|(\dot{\xi} - \dot{w}) + \gamma_3 w^3\right] = C_I\ddot{\xi}. \tag{26}$$

In this equation the effect of the cable's drag force is not explicitly included. However, its inclusion does not alter substantially the mathematical nature of the problem considered. In fact, as it is shown in Appendix A, the presence of the cable's drag force produces an additional term resulting in a quadratic form in terms of $\dot{w}_c$ with coefficients that are random processes. Therefore the cable's drag force introduces an expression that is similar to the dock's drag force.

Eq. (26) is an ordinary differential equation with two nonlinear terms (the terms in square brackets on the left-hand side) and a random input (on the right-hand side). The statistics of the displacement w can be obtained via a Monte-Carlo technique. Eq. (26) should be solved assuming different realizations of the set of the random phase angles φ_n (see Eqs. (21) and (22)). For each realization, a numerical solution is obtained and ensemble averages can be calculated. Alternatively, assuming an ergodic process, a single realization can be considered but simulated for a time long enough. The statistical moments of the solution can be calculated in this case by time averages.

With the positions:

$$\zeta = \xi - w, \quad m = m_b + m_a, \quad a_1 = \frac{2\tilde{c}}{m}, \quad a_2 = \frac{\gamma_1}{m}, \quad a_3 = \frac{C_D}{m}, \quad a_4 = \frac{\gamma_3}{m}, \quad a_5 = \frac{C_I}{m} \tag{27}$$

and substituting Eq. (27) in Eq. (26):

$$\ddot{\zeta} + a_1\dot{\zeta} + (a_2 + 3a_4\xi^2)\zeta + \left[a_3|\dot{\zeta}|\dot{\zeta} - 3a_4\xi\zeta^2 + a_4\zeta^3\right] = f(\xi), \tag{28}$$

where

$$f(\xi) = (1 - a_5)\ddot{\xi} + a_1\dot{\xi} + a_4\xi^3 + a_2\xi \tag{29}$$

is the new forcing term.

Assuming $\xi(t)$ a white noise random signal, the force f is also a white noise signal with constant power spectral density S_{f0}. If the Pierson–Moskowitz spectrum is considered, the force is indeed characterized by a frequency-dependent power spectral density.

5. Statement of the mathematical problem

Eq. (28) is a stochastic nonlinear ordinary differential equation. Instead of solving it using a Monte-Carlo simulation, different techniques of solution are proposed here able to provide directly the desired statistical moments of the dock displacement.

A first procedure, called CPSP, uses at a first step a conventional perturbation technique (CP) to produce a cascade of linear differential problems with stochastic coefficients. The second step of the procedure consists indeed in a stochastic perturbation technique (SP) to solve the obtained set of equations.

An alternative technique, called SLSP, uses at a first step a statistical linearization method (SL), followed by a SP technique.

The CPSP method leads to reasonable results only if Eq. (28) exhibits weak nonlinearity, for which the conventional perturbation technique is successful. The second part of the solution, based on a stochastic perturbation technique, can be achieved if the randomness of the coefficients is small.

The SLSP method produces at the first step a linear differential equation, in a statistical sense, equivalent to Eq. (28). The statistical linearization applies even for non-weak nonlinearities making this second approach less restrictive with respect to the CPSP method. The new equivalent equation is still a stochastic differential equation because of the random coefficients. However, since the second part of the solution is still based on a stochastic perturbation technique, again the restriction of small random coefficients holds.

6. The CPSP method

Eq. (28) is rewritten as

$$\ddot{\zeta} + a_1\dot{\zeta} + \beta(\xi)\zeta + \varepsilon g(\dot{\zeta}, \zeta, \xi) = f(t), \tag{30}$$

where

$$\beta(\xi) = a_2 + 3a_4\xi^2, \quad g(\dot{\zeta}, \zeta, \xi) = a_3|\dot{\zeta}|\dot{\zeta} - 3a_4\xi\zeta^2 + a_4\zeta^3. \tag{31}$$

Physically ε controls the cable nonlinearities and the fluid–structure interaction (drag effect) and is assumed to be small with respect to the linear contributions at least for small oscillations of the dock. The first part of the approach (CP) expands the solution in terms of power of ε up to the second order:

$$\zeta(\xi, t, \varepsilon) = \zeta_0(\xi, t) + \varepsilon\zeta_1(\xi, t) + \varepsilon^2\zeta_2(\xi, t). \tag{32}$$

$\zeta_0(\xi, t)$ is the zero-order approximation, i.e. the solution of Eq. (30) for $\varepsilon = 0$. Let expand g in terms of ε:

$$\begin{aligned} g(\dot{\zeta}, \zeta, \xi) &= g|_{\varepsilon=0} + \varepsilon g_{,\varepsilon}|_{\varepsilon=0} + \frac{\varepsilon^2}{2} g_{,\varepsilon\varepsilon}\big|_{\varepsilon=0} + O(\varepsilon^3) \\ &= g|_{\varepsilon=0} + \varepsilon\left(\dot{\zeta}_1 g_{,\dot{\zeta}}\Big|_{\varepsilon=0} + \zeta_1 g_{,\zeta}|_{\varepsilon=0}\right) \\ &\quad + \frac{\varepsilon^2}{2}\left(\dot{\zeta}_2 g_{,\dot{\zeta}}\Big|_{\varepsilon=0} + \zeta_2 g_{,\zeta}|_{\varepsilon=0} + \frac{1}{2}\zeta_1^2 g_{,\dot{\zeta}\dot{\zeta}}\Big|_{\varepsilon=0} + \frac{1}{2}\zeta_1^2 g_{,\zeta\zeta}|_{\varepsilon=0} + \dot{\zeta}_1\zeta_1 g_{,\dot{\zeta}\zeta}\Big|_{\varepsilon=0}\right) + O(\varepsilon^3). \end{aligned} \tag{33}$$

Using Eqs. (32), (33) and (30), the following equation is obtained:

$$\begin{aligned} &\ddot{\zeta}_0 + a_1\dot{\zeta}_0 + \beta(\xi)\zeta_0 + \varepsilon(\ddot{\zeta}_1 + a_1\dot{\zeta}_1 + \beta(\xi)\zeta_1) + \varepsilon^2(\ddot{\zeta}_2 + a_1\dot{\zeta}_2 + \beta(\xi)\zeta_2) \\ &\quad + \varepsilon g|_{\varepsilon=0} + \varepsilon^2\left(\dot{\zeta}_1 g_{,\dot{\zeta}}\Big|_{\varepsilon=0} + \zeta_1 g_{,\zeta}|_{\varepsilon=0}\right) \\ &\quad + \frac{\varepsilon^3}{2}\left(\dot{\zeta}_2 g_{,\dot{\zeta}}\Big|_{\varepsilon=0} + \zeta_2 g_{,\zeta}|_{\varepsilon=0} + \frac{1}{2}\dot{\zeta}_1^2 g_{,\dot{\zeta}\dot{\zeta}}\Big|_{\varepsilon=0} + \frac{1}{2}\zeta_1^2 g_{,\zeta\zeta}|_{\varepsilon=0} + \dot{\zeta}_1\zeta_1 g_{,\dot{\zeta}\zeta}\Big|_{\varepsilon=0}\right) = f(\xi). \end{aligned} \tag{34}$$

Thus, including the terms up to the second order of ε, the following cascade of linear stochastic differential equations is obtained:

$$\begin{aligned}
&\ddot{\zeta}_0 + a_1\dot{\zeta}_0 + a_2\zeta_0 + 3a_4\xi^2\zeta_0 = (1-a_5)\ddot{\xi} + a_1\dot{\xi} + a_4\xi^3 + a_2\xi,\\
&\ddot{\zeta}_1 + a_1\dot{\zeta}_1 + a_2\zeta_1 + 3a_4\xi^2\zeta_1 = 3a_4\xi\zeta_0^2 - a_3|\dot{\zeta}_0|\dot{\zeta}_0 - a_4\zeta_0^3,\\
&\ddot{\zeta}_2 + a_1\dot{\zeta}_2 + a_2\zeta_2 + 3a_4\xi^2\zeta_2 = 6a_4\xi\zeta_0\zeta_1 - 2a_3|\dot{\zeta}_0|\dot{\zeta}_1 - 3a_4\zeta_0^2\zeta_1.
\end{aligned} \tag{35}$$

The second part of the CPSP approach uses a stochastic perturbation technique to solve Eq. (35). Since $\xi = B_n\chi_n(t)$ see Eq. (21) (summation with respect to the repeated index is tacitly assumed), the solution of system (35) can be expanded in terms of the coefficients B_n, provided that they are small random parameters, as

$$\zeta_i = \zeta_{i0}(t) + B_n\zeta_{i1n}(t) + B_nB_m\zeta_{i2nm}(t). \tag{36}$$

Substitution of Eq. (36) into Eq. (35) produces, the following system (see Appendix B):

$$\begin{cases}
\ddot{\zeta}_{00} + a_1\dot{\zeta}_{00} + a_2\zeta_{00} = 0,\\
\ddot{\zeta}_{01n} + a_1\dot{\zeta}_{01n} + a_2\zeta_{01n} = (1-a_5)\ddot{\chi}_n + a_1\dot{\chi}_n + a_2\chi_n,\\
\ddot{\zeta}_{02nm} + a_1\dot{\zeta}_{02nm} + a_2\zeta_{02nm} = -3a_4\chi_n\chi_m\zeta_{00},
\end{cases} \tag{37}$$

$$\begin{cases}
\ddot{\zeta}_{10} + a_1\dot{\zeta}_{10} + a_2\zeta_{10} = -a_3|\dot{\zeta}_{00}|\dot{\zeta}_{00} - a_4\dot{\zeta}_{00}^3,\\
\ddot{\zeta}_{11n} + a_1\dot{\zeta}_{11n} + a_2\zeta_{11n} = -2a_3|\dot{\zeta}_{00}|\dot{\zeta}_{01n} - 3a_4(\dot{\zeta}_{00}^2\dot{\zeta}_{01n} + \zeta_{00}\chi_n),\\
\ddot{\zeta}_{12nm} + a_1\dot{\zeta}_{12nm} + a_2\zeta_{12nm} = 3a_4[\zeta_{01n}\chi_n - \dot{\zeta}_{00}(\dot{\zeta}_{01n}\dot{\zeta}_{01m} + \dot{\zeta}_{00}\dot{\zeta}_{02nm})]\\
-a_3|\dot{\zeta}_{00}|\left(\frac{1}{\dot{\zeta}_{00}}\dot{\zeta}_{01n}\dot{\zeta}_{01m} + 2\dot{\zeta}_{02nm}\right),
\end{cases} \tag{38}$$

$$\begin{cases}
\ddot{\zeta}_{20} + a_1\dot{\zeta}_{20} + a_2\zeta_{20} = -2a_3|\dot{\zeta}_{00}|\dot{\zeta}_{01} - 3a_4\zeta_{00}^2\zeta_{10},\\
\ddot{\zeta}_{21n} + a_1\dot{\zeta}_{21n} + a_2\zeta_{21n} = -2a_3|\dot{\zeta}_{00}|(\dot{\zeta}_{10}\dot{\zeta}_{01n}/\dot{\zeta}_{00} + \dot{\zeta}_{11n})\\
-3a_4\zeta_{00}(\zeta_{00}\zeta_{11n} + 2\zeta_{10}\zeta_{01n} + 2\zeta_{10}\chi_n),\\
\ddot{\zeta}_{22nm} + a_1\dot{\zeta}_{22nm} + a_2\zeta_{22nm} = -a_3\frac{|\dot{\zeta}_{00}|}{\dot{\zeta}_{00}}(2\dot{\zeta}_{10}\dot{\zeta}_{02nm} + \dot{\zeta}_{01n}\dot{\zeta}_{11m} + \dot{\zeta}_{11n}\dot{\zeta}_{01m} + 2\dot{\zeta}_{00}\dot{\zeta}_{12nm})\\
-3a_4[\zeta_{00}^2\zeta_{12nm} + \zeta_{10}\zeta_{01n}\zeta_{01m} + 2\zeta_{00}\zeta_{01n}\zeta_{11n} - 2\chi_n(\zeta_{00}\zeta_{11n} + \zeta_{01n}\zeta_{10})].
\end{cases} \tag{39}$$

This is a set of linear deterministic differential equations. Although their form seems complicated, if homogeneous initial conditions are assumed, a closed form solution is readily obtained. In fact, in this case, the first of Eq. (37), and consequently the third, have void solutions: $\zeta_{00} = 0$ and $\zeta_{02nm} = 0$. Likewise, the first and the second equations of (38) have void right-hand terms, then $\zeta_{10} = 0$ and $\zeta_{11n} = 0$. Eq. (39) has all the right-hand terms void. Thus,

$$\begin{cases}
\ddot{\zeta}_{01n} + a_1\dot{\zeta}_{01n} + a_2\zeta_{01n} = (1-a_5)\ddot{\chi}_n + a_1\dot{\chi}_n + a_2\chi_n,\\
\ddot{\zeta}_{12nm} + a_1\dot{\zeta}_{12nm} + a_2\zeta_{12nm} = 3a_4\zeta_{01n}\chi_m - a_3\dot{\zeta}_{01n}\dot{\zeta}_{01m}.
\end{cases} \tag{40}$$

Using Eq. (36), the solution of (40) produces

$$\zeta_0 = B_n\zeta_{01n}(t), \quad \zeta_1 = B_nB_m\zeta_{12nm}(t) \tag{41}$$

and (see Eq. (32))

$$\zeta(\xi, t, \varepsilon) = B_n\zeta_{01n}(t) + \varepsilon B_nB_m\zeta_{12nm}(t). \tag{42}$$

Since the B's are statistically independent, the second-order statistical moment of the relative displacement (42) can be calculated as follows:

$$E\{\zeta^2\} = \sum_{n=-\infty}^{\infty} \left(E\{B_n B_m^*\}\zeta_{01n}\zeta_{01n}^*\right) + O(B_n^3). \tag{43}$$

Looking at the steady-state response and using Eqs. (21) and (22), the solution of the first equation of (40) is

$$\zeta_{01n}(t) = \frac{-\omega_n^2(1-a_5) + \mathrm{j}\omega_n a_1 + a_2}{-\omega_n^2 + \mathrm{j}\omega_n a_1 + a_2} \mathrm{e}^{\mathrm{j}\omega_n t} \tag{44}$$

and finally

$$E\{\zeta^2\} = \sum_{n=-\infty}^{\infty} \left(E\{B_n B_m^*\}\left|\frac{-\omega_n^2(1-a_5) + \mathrm{j}\omega_n a_1 + a_2}{-\omega_n^2 + \mathrm{j}\omega_n a_1 + a_2}\right|^2\right) + O(B_n^3). \tag{45}$$

7. The SLSP method

In this section the SLSP method is presented. In Section 7.1 some basic elements of statistical linearization are illustrated. Section 7.2 applies the general theory to the case of the dock equation and in Section 7.3 the case of a Gaussian statistics, for which closed form solution are found, is eventually considered.

7.1. Brief notes on statistical linearization

The basic ideas of the statistical linearization relies in replacing a nonlinear system by an "equivalent" linear one so that the difference between the response of the two systems is minimal in some probabilistic sense [12,18–21]. More precisely, it is required that the mean-square difference between the nonlinear forces and their counterpart in the equivalent linear systems be minimum.

Consider the equation:

$$\mathscr{L}(x, \dot{x}, t) + \mathscr{N}\mathscr{L}(x, \dot{x}, t) = f(t), \tag{46}$$

where $\mathscr{N}\mathscr{L}(x, \dot{x}, t)$ and $\mathscr{L}(x, \dot{x}, t)$ are the nonlinear and the linear part of the system's operator, respectively, $x(t)$ is the system's response and $f(t)$ an external random force. A linear operator $\mathscr{L}_{\mathrm{eq}}(y, \dot{y}, \mathsf{p}, t)$ can replace $\mathscr{N}\mathscr{L}$ in the sense of SL, where $y(t)$ is the system's response of the linear equivalent system and p a vector of unknown parameters:

$$\mathscr{L}(y, \dot{y}, t) + \mathscr{L}_{\mathrm{eq}}(y, \dot{y}, \mathsf{p}, t) = f(t). \tag{47}$$

Adding the term $\mathscr{L}_{\mathrm{eq}}$ to both sides of Eq. (46), rearranging and assuming $x(t) = y(t)$ the following equation may be written:

$$\mathscr{L}(x, \dot{x}, t) + \mathscr{L}_{\mathrm{eq}}(x, \dot{x}, \mathsf{p}, t) = f(t) + \mathscr{E}(x, \dot{x}, \mathsf{p}, t), \tag{48}$$

where

$$\mathscr{E}(x, \dot{x}, \mathsf{p}, t) = \mathscr{L}_{\mathrm{eq}}(x, \dot{x}, \mathsf{p}, t) - \mathscr{N}\mathscr{L}(x, \dot{x}, t) \tag{49}$$

which is the equation error.

The unknown parameters p are determined minimizing the mean-square of $\mathscr{E}$:

$$\frac{\partial E\{\mathscr{E}^2\}}{\partial \mathsf{p}} = 0. \tag{50}$$

The expectations in Eq. (50) should be evaluated ideally using the exact joint probability density function (pdf) $p(x, t; \dot{x}, t)$ of the nonlinear response $x(t)$ and of its derivative $\dot{x}(t)$.

If the exact probability distribution is used to evaluate Eq. (50), then the variance $E\{y^2\}$ would be exactly equal to $E\{x^2\}$.

However, this pdf is, in general, unknown and, a trial function is indeed considered to calculate the statistical moment which are the coefficients of Eq. (50). The choice of this approximated pdf depends on the input pdf and on the nonlinearities of the governing equation.

7.2. Statistical linearization of the dock equation

Applying the method described in the previous section to Eq. (28), the new governing equation is

$$\ddot{\zeta} + (a_1 + c_{\mathrm{SLeq}})\dot{\zeta} + (a_2 + 3a_4\xi^2 + k_{\mathrm{SLeq}})\zeta = f(\xi). \tag{51}$$

The parameters c_{SLeq} and k_{SLeq} are calculated by the solution of the problem shown in Eq. (50).

The equation error $\mathscr{E}$ between Eqs. (28) and (51) is

$$\mathscr{E} = c_{\mathrm{SLeq}}\dot{\zeta} + k_{\mathrm{SLeq}}\zeta - \left[a_3|\dot{\zeta}|\dot{\zeta} - 3a_4\xi\zeta^2 + a_4\zeta^3\right] \tag{52}$$

and the two following equations can be written:

$$\begin{cases} \partial E\{\mathscr{E}^2\}/\partial c_{\mathrm{SLeq}} = 0, \\ \partial E\{\mathscr{E}^2\}/\partial k_{\mathrm{SLeq}} = 0 \end{cases} \tag{53}$$

or explicitly:

$$\begin{cases} c_{\mathrm{SLeq}}E\{\dot{\zeta}^2\} + k_{\mathrm{SLeq}}E\{\dot{\zeta}\zeta\} = a_3E\{|\dot{\zeta}|\dot{\zeta}^2\} + 3a_4\xi E\{\dot{\zeta}\zeta^2\} + a_4E\{\dot{\zeta}\zeta^3\}, \\ c_{\mathrm{SLeq}}E\{\dot{\zeta}\zeta\} + k_{\mathrm{SLeq}}E\{\zeta^2\} = a_3E\{|\dot{\zeta}|\dot{\zeta}\zeta\} + 3a_4\xi E\{\zeta^3\} + a_4E\{\zeta^4\} \end{cases} \tag{54}$$

in the unknowns c_{SLeq} and k_{SLeq}.

Assuming the solution process $\zeta(t)$ and its derivative $\dot{\zeta}(t)$ stationary statistically, independent and with zero mean, then

$$E\{\zeta^3\} = 0, \quad E\{\dot{\zeta}\zeta\} = E\{\dot{\zeta}\zeta^2\} = E\{\dot{\zeta}\zeta^3\} = 0. \tag{55}$$

The solution of Eq. (54) is

$$c_{\mathrm{SLeq}} = a_3\frac{E\{|\dot{\zeta}|\dot{\zeta}^2\}}{E\{\dot{\zeta}^2\}}, \quad k_{\mathrm{SLeq}} = \frac{a_3E\{|\dot{\zeta}|\dot{\zeta}\zeta\} + a_4E\{\zeta^4\}}{E\{\zeta^2\}}. \tag{56}$$

We can proceed further in the analysis illustrating in the next section the second part of the SLSP, under the hypothesis of Gaussian statistics.

7.3. Gaussian statistics and the statistical perturbation technique

Assumed the force on the floating buoy Gaussian, $\zeta(t)$ and $\dot{\zeta}(t)$ are also normal processes, stationary and statistically independent with joint pdf:

$$p_n(\zeta, \dot{\zeta}) = \frac{1}{\sigma_\zeta\sigma_{\dot{\zeta}}\sqrt{2\pi}}\mathrm{e}^{-(\zeta/\sigma_\zeta^2 + \dot{\zeta}/\sigma_{\dot{\zeta}}^2)/2}. \tag{57}$$

The coefficients in Eq. (56) can be determined using the properties of the Gaussian processes. Hence

$$E\{|\dot{\zeta}|\dot{\zeta}\zeta\} = 0 \tag{58}$$

and by the Kazakov's theorem [12]:

$$\frac{E\{|\dot{\zeta}|\dot{\zeta}^2\}}{E\{\dot{\zeta}^2\}} = \frac{E\{\dot{\zeta}^2\}E\{(|\dot{\zeta}|\dot{\zeta})'\}}{E\{\dot{\zeta}^2\}} = E\{(|\dot{\zeta}|\dot{\zeta})'\}, \tag{59}$$

where apex indicates the derivative with respect to $\dot{\zeta}$. Expectation in Eq. (59) may be evaluated in closed form:

$$E\{(|\dot{\zeta}|\dot{\zeta})'\} = \sqrt{\frac{8}{\pi}}\sigma_{\dot{\zeta}}. \tag{60}$$

Therefore, Eq. (56) may be rewritten as follows:

$$c_{\mathrm{SLeq}} = a_3\sqrt{\frac{8}{\pi}}\sigma_{\dot{\zeta}}, \quad k_{\mathrm{SLeq}} = 3a_4\sigma_{\zeta}^2. \tag{61}$$

Substitution for these coefficients in Eq. (51) produces

$$\ddot{\zeta} + (a_1 + a_3\sqrt{8/\pi}\sigma_{\dot{\zeta}})\dot{\zeta} + (a_2 + 3a_4\xi^2 + 3a_4\sigma_{\zeta}^2)\zeta = f(\xi). \tag{62}$$

Eq. (62) is a linear ordinary differential equation with the random coefficient $3a_4\xi^2$. Moreover, the coefficients $a_3\sqrt{8/\pi}\sigma_{\dot{\zeta}}$ and $3a_4\sigma_{\zeta}^2$ depend on the statistical moments of the solution.

The second step of the SLSP procedure, the stochastic perturbation technique, relies on the series expansion (21). Analogously to Eq. (36), ζ is expanded in terms of the coefficients B_n:

$$\zeta(t) = \zeta_0(t) + B_n\zeta_{1n}(t) + B_nB_m\zeta_{2nm}(t) \tag{63}$$

that substituted in Eq. (62) produces

$$\begin{aligned}&\ddot{\zeta}_0 + B_n\ddot{\zeta}_{1n} + B_nB_m\ddot{\zeta}_{2nm} + (a_1 + a_3\sqrt{8/\pi}\sigma_{\dot{\zeta}})(\dot{\zeta}_0 + B_n\dot{\zeta}_{1n} + B_nB_m\dot{\zeta}_{2nm})\\ &\quad + (a_2 + 3a_4B_nB_m\chi_n\chi_m + 3a_4\sigma_{\zeta}^2)(\zeta_0 + B_n\zeta_{1n} + B_nB_m\zeta_{2nm}) = (1-a_5)\ddot{\chi}_n + a_1\dot{\chi}_n + a_2\chi_n\end{aligned} \tag{64}$$

Separating the different orders of the B's, the following set of linear independent differential equations is obtained:

$$\begin{cases}\ddot{\zeta}_0 + (a_1 + a_3\sqrt{8/\pi}\sigma_{\dot{\zeta}})\dot{\zeta}_0 + (a_2 + 3a_4\sigma_{\zeta}^2)\zeta_0 = 0,\\ \ddot{\zeta}_{1n} + (a_1 + a_3\sqrt{8/\pi}\sigma_{\dot{\zeta}})\dot{\zeta}_{1n} + (a_2 + 3a_4\sigma_{\zeta}^2)\zeta_{1n} = (1-a_5)\ddot{\chi}_n + a_1\dot{\chi}_n + a_2\chi_n,\\ \ddot{\zeta}_{2nm} + (a_1 + a_3\sqrt{8/\pi}\sigma_{\dot{\zeta}})\dot{\zeta}_{2nm} + (a_2 + 3a_4\sigma_{\zeta}^2)\zeta_{2nm} = 0.\end{cases} \tag{65}$$

When void initial conditions are considered, the zero and second order give void the solutions $\zeta_0 = 0$ and $\zeta_{2nm} = 0$. The first-order solutions, ζ_{1n}, are sufficient to obtain the relative displacement:

$$\zeta(t) = B_n\zeta_{1n}(t). \tag{66}$$

The standard deviation of the relative velocity and the variance of the relative displacement are in general unknowns, because they are nonlinear functions of the equation unknowns. When the random input is a white noise, the force power spectral density is constant and a closed form for the variance can be obtained.

Unfortunately, thus is not true in case the power spectral density is not constant as, for example, for the Pierson–Moskowitz spectrum.

Let conclude with an approximate iterative solution of the problem. Eqs. (21) and (22) can be considered a rough approximation of Eq. (65). Neglecting the terms containing statistical moments, $\zeta_{1n}^{(0)}$ can be approximated as

$$\zeta_{1n}^{(0)}(t) = \frac{-\omega_n^2(1-a_5) + \mathrm{j}\omega_n a_1 + a_2}{-\omega_n^2 + \mathrm{j}\omega_n a_1 + a_2}\mathrm{e}^{\mathrm{j}\omega_n t}. \tag{67}$$

Therefore, from Eq. (66):

$$\zeta^{(0)}(t) = \left[B_n\frac{-\omega_n^2(1-a_5) + \mathrm{j}\omega_n a_1 + a_2}{-\omega_n^2 + \mathrm{j}\omega_n a_1 + a_2}\right]\mathrm{e}^{\mathrm{j}\omega_n t}. \tag{68}$$

An estimate of the variance is obtained from Eq. (68):

$$\sigma_{\zeta}^{2(0)} = E\{\zeta^{(0)}\zeta^{*(0)}\} = E\{B_nB_m^*\}\left|\frac{-\omega_n^2(1-a_5) + \mathrm{j}\omega_n a_1 + a_2}{-\omega_n^2 + \mathrm{j}\omega_n a_1 + a_2}\right|^2. \tag{69}$$

This expression can be used to start an iterative procedure in which the statistical moments calculated at the previous step allow to achieve the solution at the new iteration. Therefore, the steady-state solution of Eq. (65) is

$$\zeta_{1n}^{(i)}(t) = \frac{-\omega_n^2(1-a_5) + \mathrm{j}\omega_n a_1 + a_2}{-\omega_n^2 + \mathrm{j}\omega_n(a_1 + a_3\sqrt{8/\pi}\sigma_{\dot\zeta}^{(i-1)}) + (a_2 + 3a_4\sigma_\zeta^{2(i-1)})} \mathrm{e}^{\mathrm{j}\omega_n t}. \tag{70}$$

Eq. (66) provides:

$$\zeta^{(i)}(t) = \left[B_n \frac{-\omega_n^2(1-a_5) + \mathrm{j}\omega_n a_1 + a_2}{-\omega_n^2 + \mathrm{j}\omega_n(a_1 + a_3\sqrt{8/\pi}\sigma_{\dot\zeta}^{(i-1)}) + (a_2 + 3a_4\sigma_\zeta^{2(i-1)})} \right] \mathrm{e}^{\mathrm{j}\omega_n t} \tag{71}$$

and the second statistical moment:

$$\sigma_\zeta^{2(i)} = E\{\zeta^{(i)}\zeta^{*(i)}\} = E\{B_n B_m^*\} \left| \frac{-\omega_n^2(1-a_5) + \mathrm{j}\omega_n a_1 + a_2}{-\omega_n^2 + \mathrm{j}\omega_n(a_1 + a_3\sqrt{8/\pi}\sigma_{\dot\zeta}^{(i-1)}) + (a_2 + 3a_4\sigma_\zeta^{2(i-1)})} \right|^2. \tag{72}$$

This procedure can be repeated for $i = 1, 2, 3, \ldots,$ until the convergence is reached. The adopted convergence criterion involves the calculus of the relative difference between the results at iteration i and $i+1$: when this value is less than 1% the convergence is considered reached.

8. Numerical results and comparisons

The buoy considered for the numerical simulations has diameter 10 m and mass 12,000 kg. The sea depth is 50 m. The buoy is anchored by two steel cables with suspended lengths equal to 150 m. The Pierson–Moskowitz spectrum characterizes the wave spectrum, and six different wind velocities are considered: 5, 8, 10, 15, 20, 25 m/s. The corresponding spectra are represented in Fig. 4, respectively.

To check the validity of the proposed methods, a reference solution of Eq. (28) is determined by a direct numerical integration. By taking advantage of the ergodicity of the phenomenon, the statistical moments of the solution are determined by long time numerical simulations.

Figs. 5,7,9 and 11 show the phase space, the pdfs of the relative displacement and of the relative velocity and the comparison between these pdfs and the corresponding normal probability (having same mean and variance) for the wind speed 5, 10, 20 and 25 m/s, respectively. The pdfs are obtained by calculating the histogram of two perpendicular cuts of the phase space: one parallel to the displacement axis and one parallel to the velocity axis. Figs. 6,8,10 and 12 show the normal probability plot for the same quantities in order to quantify the deviation from the corresponding normal probability distribution. It appears that all the considered processes are almost Gaussian. In fact, also for large values of the wind speed, the relative displacement has a distribution that is close to be Gaussian.

Fig. 13 shows the power spectral density of ζ for the considered wind velocities. The first peak corresponds to the natural frequency of the rough linearization, $f_n = \sqrt{a_2}/2\pi = 0.036$ Hz, the second is related to the maximum of the Pierson–Moskowitz spectrum.

In Table 1 the autocorrelation R_ζ for $\tau = 0$ is compared with the variance determined by Eqs. (45) and (72), associated with the SLSP and CPSP methods, respectively, and a good agreement is observed up to a wind speed of 10 m/s. A number of iterations sufficient to guarantee the convergence of the procedure are performed. For the wind velocities 5, 8, 10, 15 and 20 m/s, seven iterations were sufficient to reach the convergence of the procedure. On the contrary for $U = 25$ m/s the variance of the displacement does not converge regularly as shown in Fig. 14. Moreover, for this last speed, the predicted variance does not match the value obtained by numerical integration of the equation of motion (see Table 1). This means that the methods are reliable at least for moderate nonlinearities and that the wind speed, i.e. the waves amplitude, should be small. The results are in acceptable agreement with the theoretical predictions with an error up to 14% at the wind speed of 10 m/s (in practice acceptable results are obtained for wind speeds less than 10 m/s).

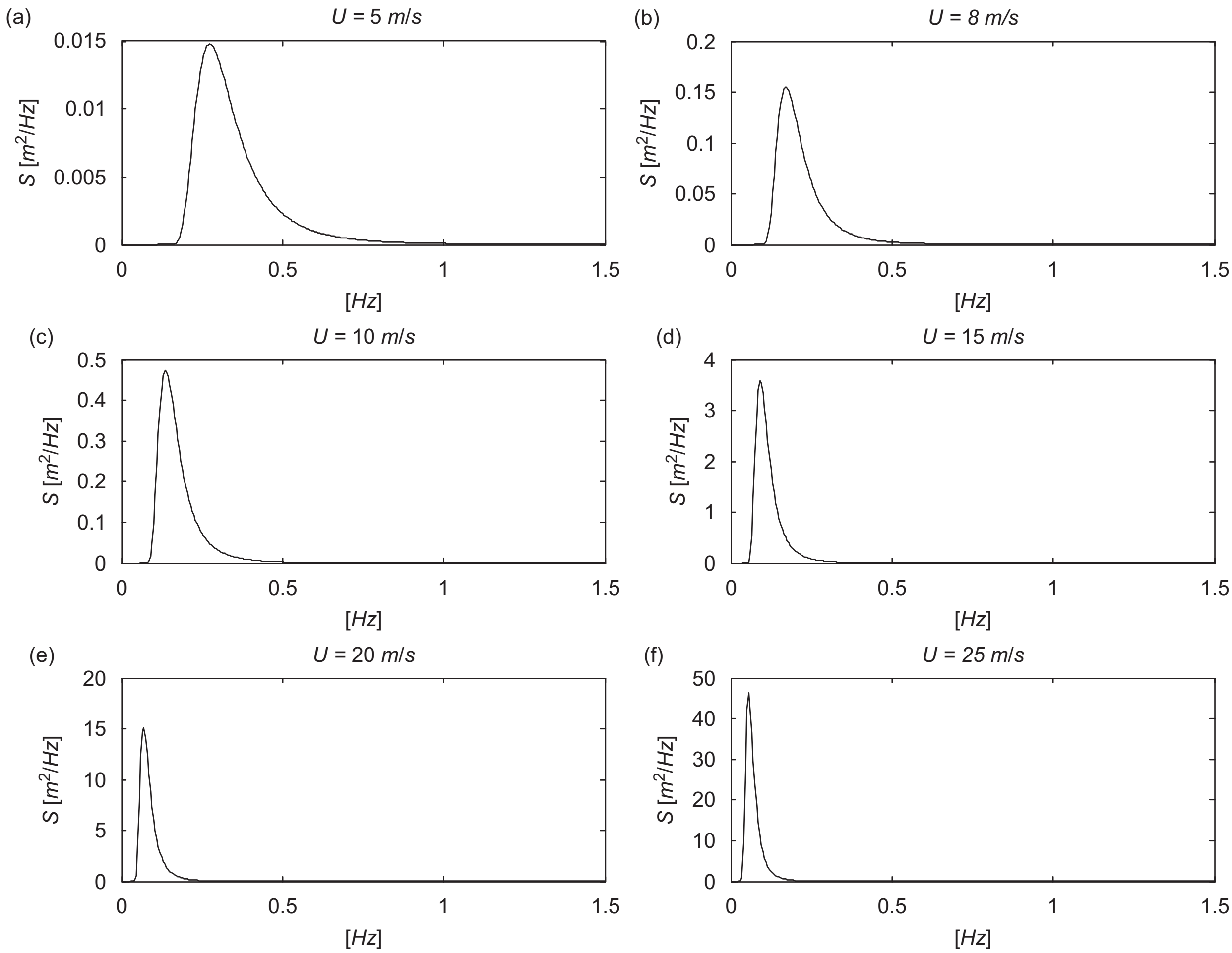

Fig. 4. Pierson—Moskowitz spectrum: (a) $U = 5\,\text{m/s}$, (b) $U = 8\,\text{m/s}$, (c) $U = 10\,\text{m/s}$, (d) $U = 15\,\text{m/s}$, (e) $U = 20\,\text{m/s}$, (f) $U = 25\,\text{m/s}$.

Looking at Figs. 5–12, it appears that the results obtained by the SLSP are a little better than those obtained by the CPSP when increasing the wind speed. The reason for this relies on the double use of the perturbation technique in the CPCS method that is more sensitive to the effect of strong nonlinearities.

9. Conclusions

This paper presents two different techniques for the analysis of differential equations with stochastic coefficient. The example of application concerns the prediction of the wave-induced oscillations of a moored vessel, but systems of different physical nature can be analysed with the same methodology.

Both methods are based on stochastic perturbation techniques. The first classical perturbation–statistical perturbation (CPSP) consists of a sequential application of a classical perturbation technique to reduce the nonlinear stochastic differential equation to a linear equation with stochastic coefficients, and of a stochastic perturbation approach to provide the statistical moments of the solution. The second technique, statistical linearization–stochastic perturbation (SLSP) is based on a statistical linearization of the nonlinear problem leading to a linear differential problem with stochastic coefficients that is eventually treated by a stochastic perturbation approach.

Both the techniques reveal their advantage in terms of computational costs with respect to direct Monte-Carlo simulations.

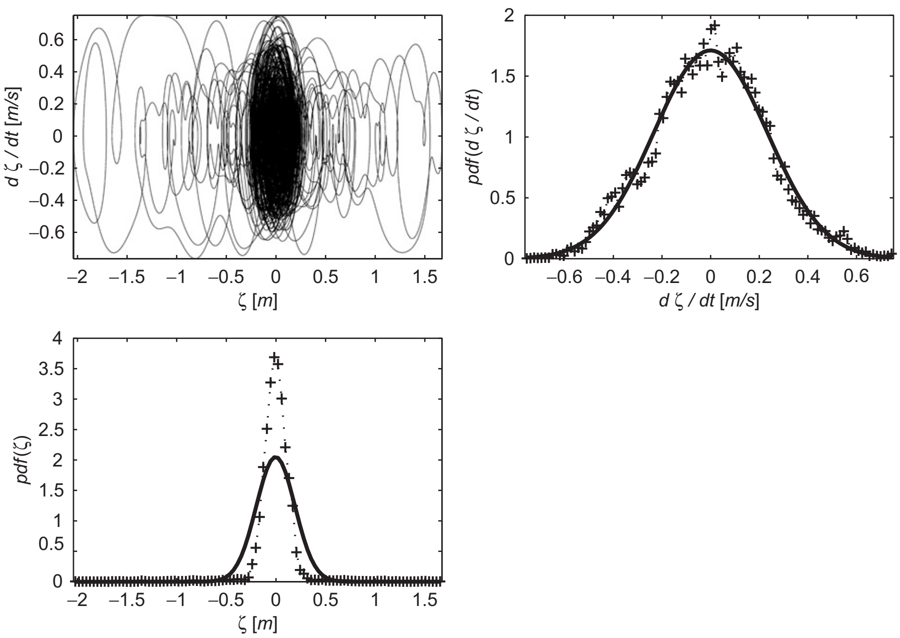

Fig. 5. Phase space and pdf of relative velocity and displacement, wind velocity 5 m/s: ⋯ + ⋯, results; ______, Gaussian pdf.

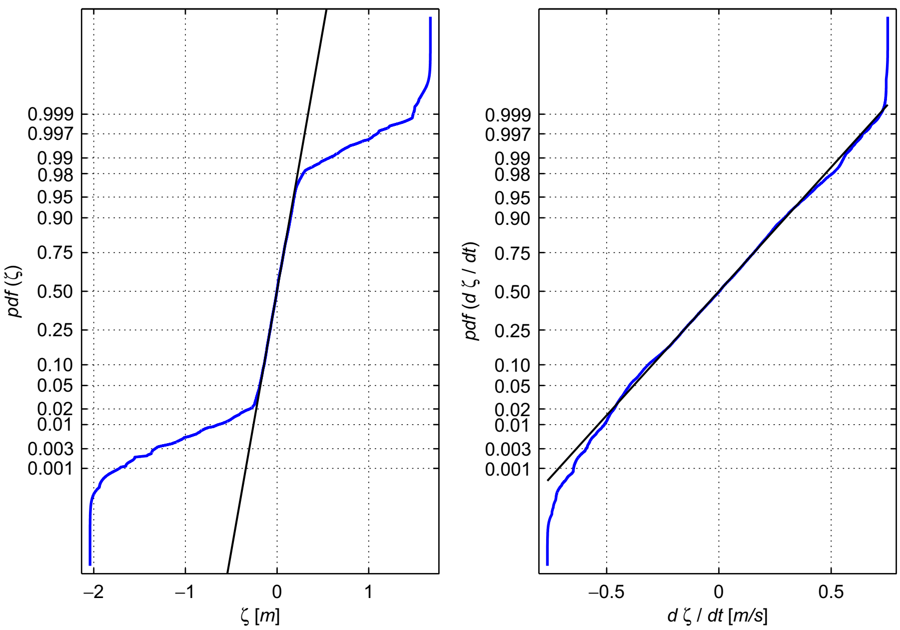

Fig. 6. Normal probability plot of relative velocity and displacement, wind velocity 5 m/s.

The methods are reliable at least for moderate nonlinearities. In the present application this means that the wind speed, i.e. the waves amplitude, should be small. The results are in acceptable agreement with the theoretical predictions with an error up to 14% at the wind speed of 10 m/s (in practice acceptable results are

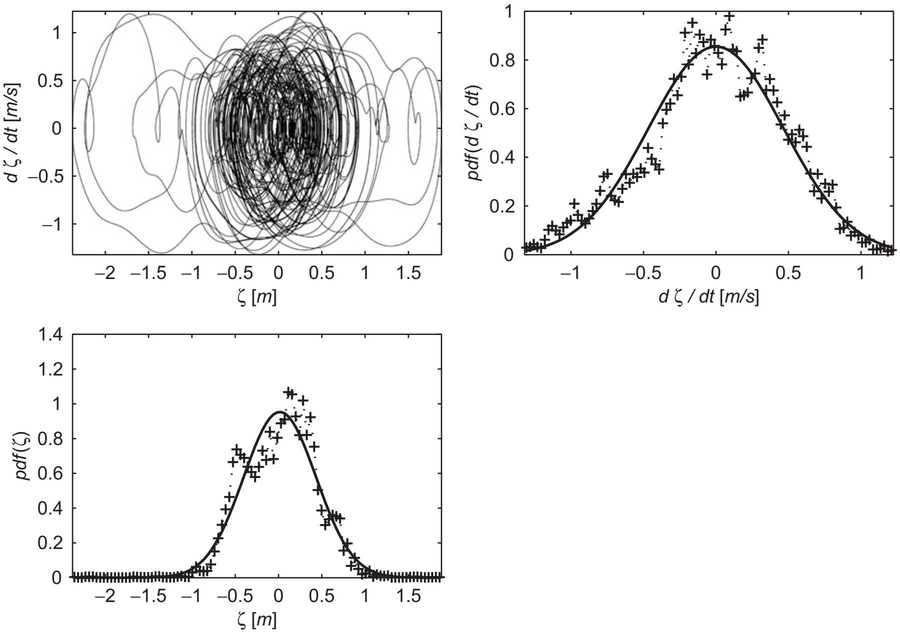

Fig. 7. Phase space and pdf of relative velocity and displacement, wind velocity 10 m/s: ⋯+⋯, results; ______, Gaussian pdf.

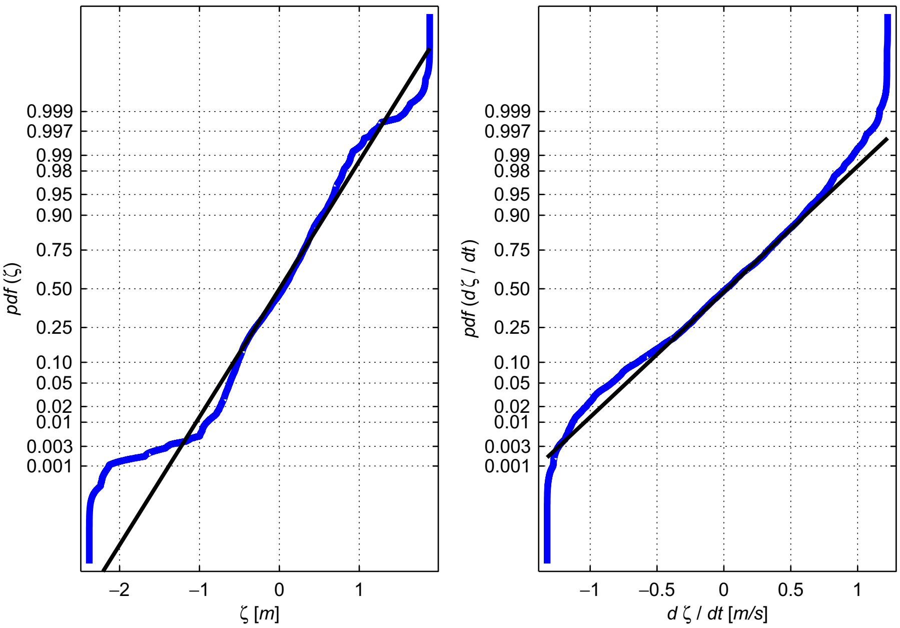

Fig. 8. Normal probability plot of relative velocity and displacement, wind velocity 10 m/s.

obtained for wind speeds less than 10 m/s). This is indeed a consequence of the perturbation approach that is valid only in the limit of small nonlinear perturbations. The SLSP method in this respect is more robust than the CPSP because the first statistical linearization approach (SL) does not need for its application small nonlinearities, while this condition is required by the second part of the method (SP) based on a stochastic perturbation.

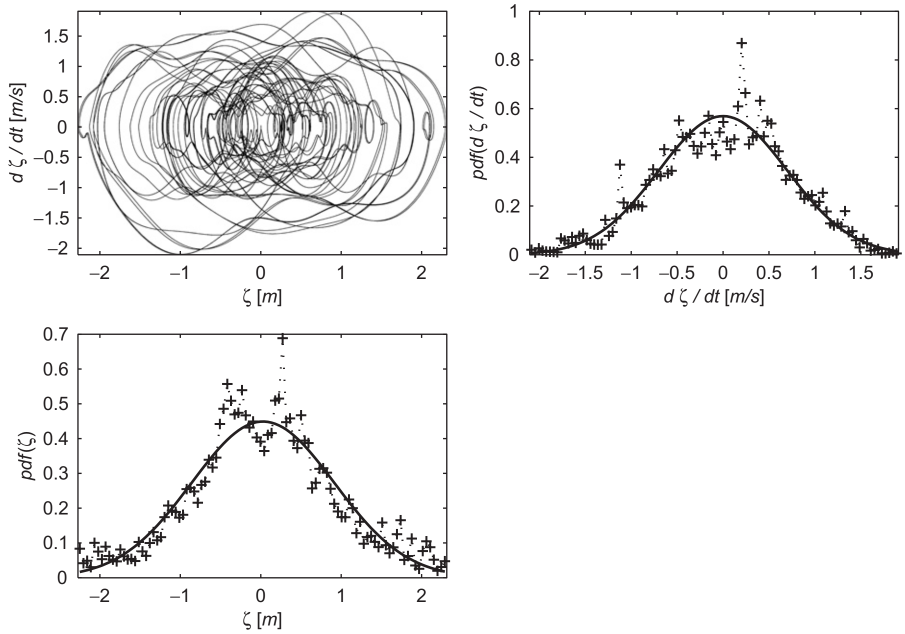

Fig. 9. Phase space and pdf of velocity and displacement, wind velocity 20 m/s: $\cdots + \cdots$, results; ______, Gaussian pdf.

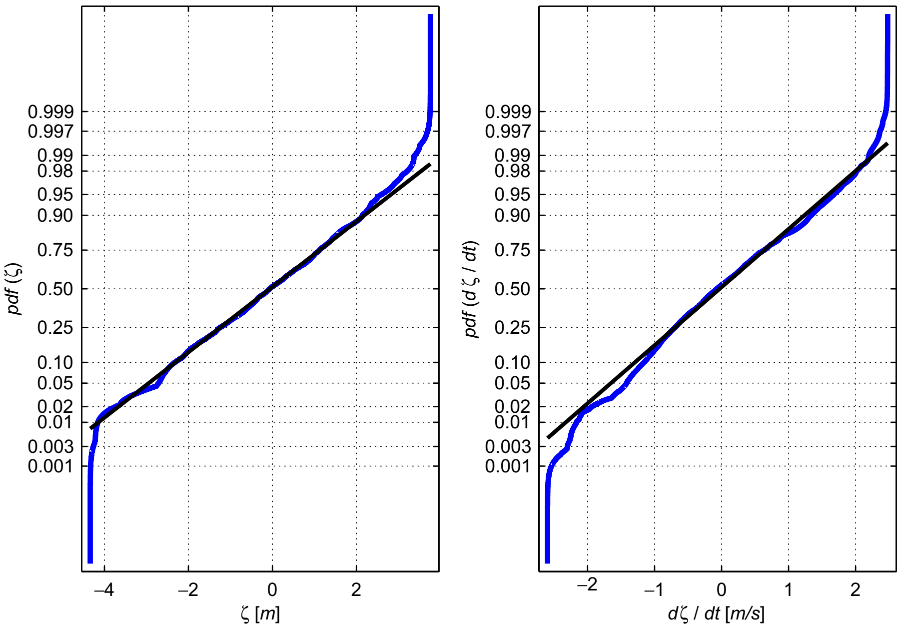

Fig. 10. Normal probability plot of relative velocity and displacement, wind velocity 20 m/s.

Appendix A

Potential water waves can be described by the Airy theory. The spectral component of the velocity potential φ at frequency ω is

$$\varphi(x,z,t) = \frac{gH\,\cosh[k(x+h)]}{2\omega\,\cosh(kh)} e^{j(kz-\omega t)}. \quad (73)$$

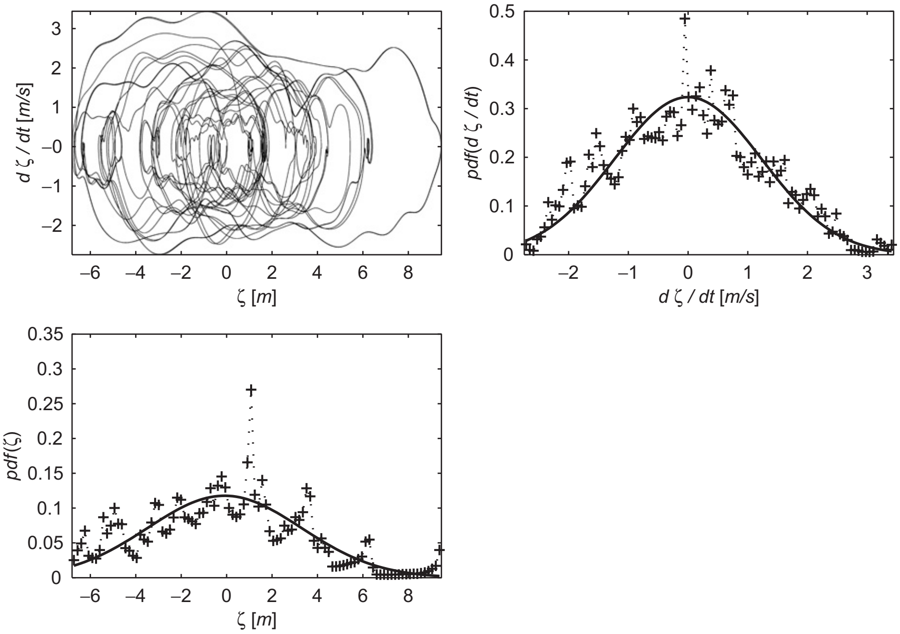

Fig. 11. Phase space and pdf of relative velocity and displacement, wind velocity 25 m/s: ⋯ + ⋯, results; ______, Gaussian pdf.

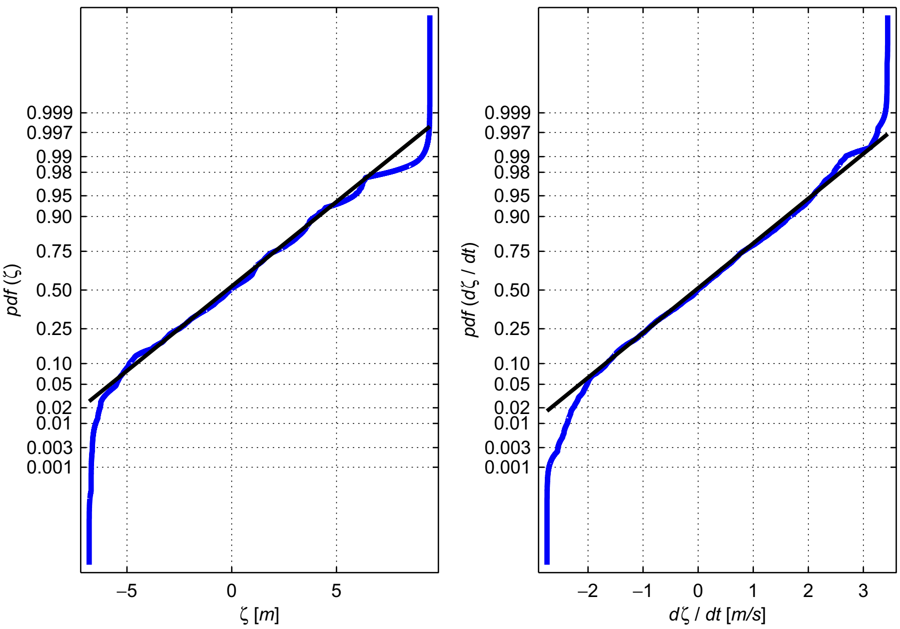

Fig. 12. Normal probability plot of relative velocity and displacement, wind velocity 25 m/s.

The related fluid particles velocity components along the x and z axes are:

$$v_{f_x} = \frac{\partial \varphi}{\partial x} \quad v_{f_z} = \frac{\partial \varphi}{\partial z}. \tag{74}$$

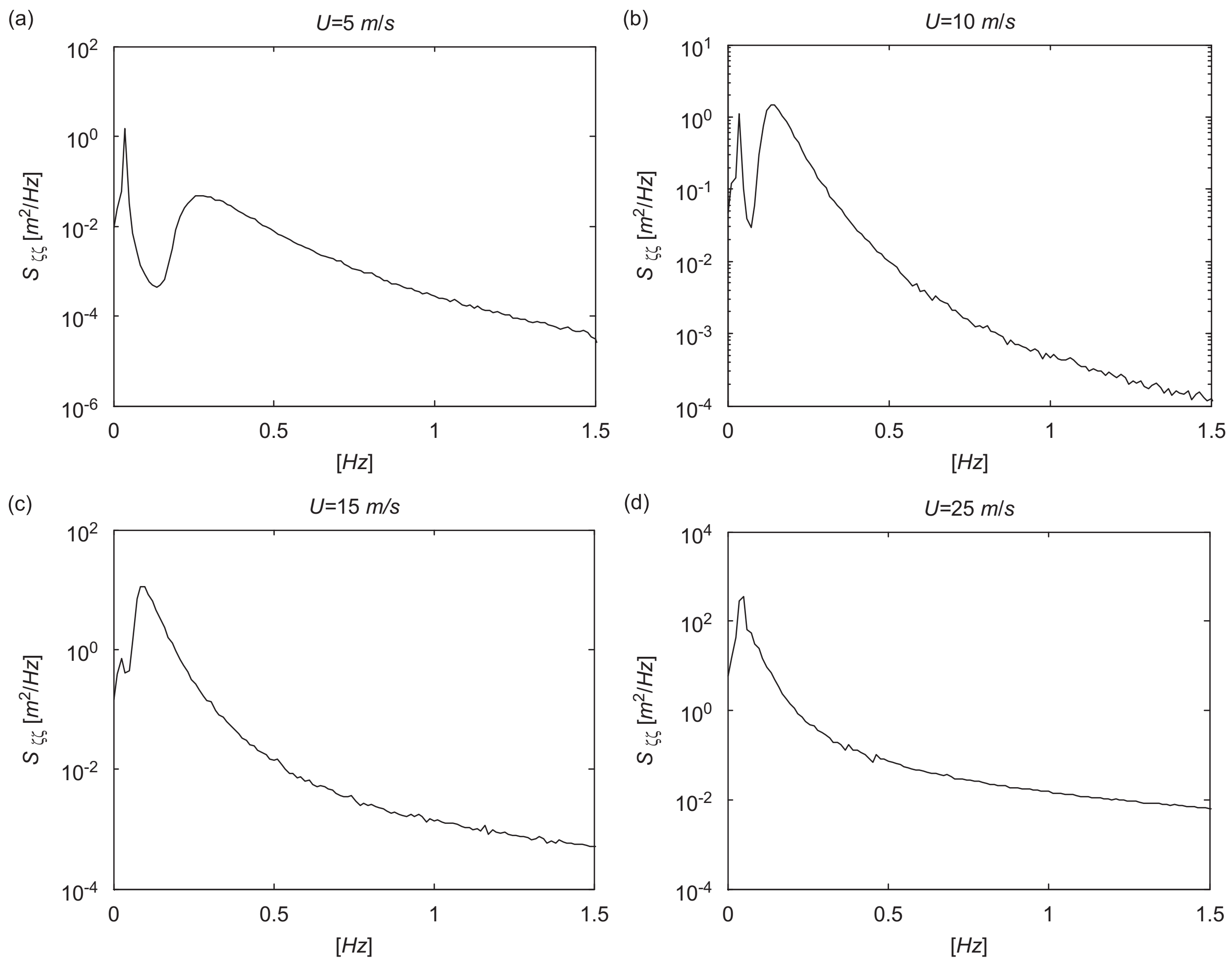

Fig. 13. Power spectral density of the response: (a) $U = 5\,\text{m/s}$, (b) $U = 10\,\text{m/s}$, (c) $U = 15\,\text{m/s}$ and (d) $U = 25\,\text{m/s}$.

Table 1
Comparison between the numerical results for different wind velocities

Wind velocity (m/s)	P.-M. spectrum freq. peak (Hz)	$R_\zeta(0)$	σ^2_{zz} CPSP	σ^2_{zz} SLSP
5	0.275	0.0098	0.01	0.01
8	0.17	0.064	0.075	0.075
10	0.135	0.153	0.202	0.201
15	0.09	0.792	1.759	1.747
20	0.07	2.77	19.23	18.77
25	0.055	11.56	828.5	67.2/34.8

These components at $x = x(s)$ and $z = z(s)$, i.e. along the cable line, are:

$$v_{f_x} = k\frac{gH\,\sinh[k(x(s)+h)]}{2\omega\,\cosh(kh)}e^{j(kz-\omega t)},$$
$$v_{f_z} = jk\frac{gH\,\cosh[k(x(s)+h)]}{2\omega\,\cosh(kh)}e^{j(kz-\omega t)} \tag{75}$$

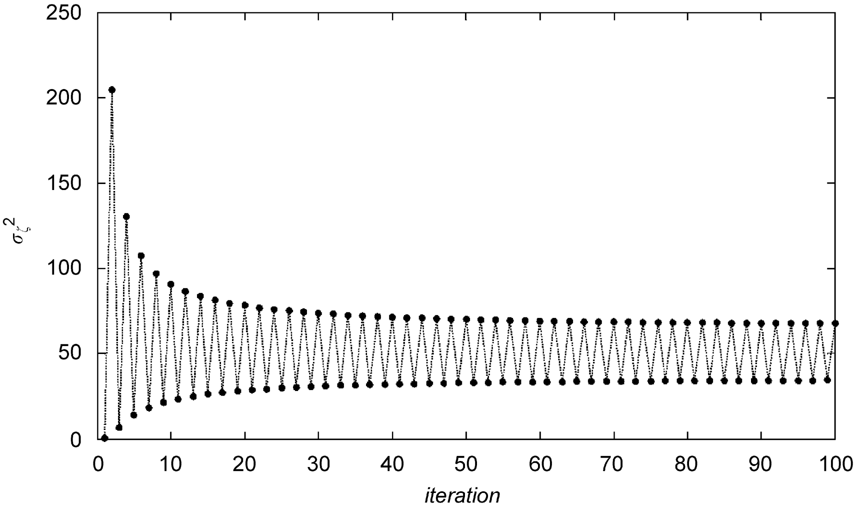

Fig. 14. Convergence of the relative displacement variance, wind velocity: 25 m/s.

or more concisely:

$$\begin{matrix} v_{f_x} = f_x(s,k)e^{j(kz-\omega t)} \\ v_{f_z} = f_z(s,k)e^{j(kz-\omega t)} \end{matrix} \leftrightarrow \underline{v}_f = \begin{bmatrix} f_x(s,k) \\ f_z(s,k) \end{bmatrix} e^{j(kz-\omega t)} = \underline{f}(s,k)e^{j(kz-\omega t)}. \tag{76}$$

The free surface waves represent a random process described by the superposition of harmonic components:

$$\underline{v}_f = \sum_{n=-\infty}^{+\infty} A_n \underline{f}(s,k_n)e^{j(k_n z-\omega t)}, \tag{77}$$

where the A_n coefficients are random complex (amplitude and phase) variables.

The velocity of the cable's points can be expressed in terms of $\dot{w}_c(t)$ using the shape functions $\psi_x(s)$ and $\psi_z(s)$ (e.g. determined on the basis of the static catenary solution) as

$$\begin{matrix} v_{c_x} = \psi_x(s)\dot{w}_c(t) \\ v_{c_z} = \psi_z(s)\dot{w}_c(t) \end{matrix} \leftrightarrow \underline{v}_c = \begin{bmatrix} \psi_x(s) \\ \psi_z(s) \end{bmatrix} \dot{w}_c(t) = \underline{\psi}(s)\dot{w}_c(t). \tag{78}$$

Thus the fluid-cable relative velocity is

$$\underline{v}_r(s,t) = \underline{v}_c - \underline{v}_f = \underline{\psi}(s)\dot{w}_c(t) - \sum_{n=-\infty}^{+\infty} A_n \underline{f}(s,k_n)e^{j(k_n z-\omega t)}. \tag{79}$$

Assuming the cable's drag force components along x and z proportional to $|\underline{v}_r|^2$ produces

$$F_{dx} = \alpha_x(s)|\underline{v}_r|^2, \quad F_{dz} = \alpha_z(s)|\underline{v}_r|^2, \tag{80}$$

where the coefficients $\alpha_x(s)$ and $\alpha_z(s)$ depend on the angle of attack of the fluid velocity with respect to the cable's local tangent that is a function of the location s.

Thus, the total drag cable force component along the z-axis is

$$R_z = \int_0^l \alpha_z(s)|\underline{v}_r(s,t)|^2 \, ds \tag{81}$$

i.e.:

$$R_z = \int_0^l \alpha_z(s)\left|\underline{\psi}(s)\dot{w}_c(t) - \sum_{n=-\infty}^{+\infty} A_n \underline{f}(s,k_n)e^{j(k_n z-\omega t)}\right|^2 ds. \tag{82}$$

That, with obvious meaning of the symbols, becomes:

$$R_z(t) = C_1(t) + C_2(t)\dot{w}_c + C_3(t)\dot{w}_c^2. \tag{83}$$

This drag force can be introduced into the dock's equation of motion. It is a quadratic form of the dock's velocity and its mathematical expression is similar to the dock's drag force appearing into Eq. (19).

Finally, the effect of a uniform current can be readily introduced by an additional potential term $\varphi_\infty(z) = U_\infty z$ in Eq. (73). Expression (83) remains in this case identical except a different value for the coefficient C_1.

Appendix B

In this appendix are shown the remarkable relationships necessary to obtain Eqs. (37)–(39) of Section 6.

Before, a set of general relationships are presented which are necessary for the following developments (Eqs. (84)–(88)). After, two Taylor's series expansions which appear in the second and third equations of Eq. (35) are developed (Eqs. (89)–(96)). Last but not the least, Eq. (35), by considering Eqs. (21) and (36) and all those developed in the appendix ((84)–(96)) are written in order to obtain Eqs. (37)–(39).

B.1. General relationships

$$\frac{\partial \dot{\zeta}_i}{\partial B_n} = \frac{\partial}{\partial B_n}(\dot{\zeta}_{i0} + B_n\dot{\zeta}_{i1n} + B_nB_m\dot{\zeta}_{i2nm}) = \dot{\zeta}_{i1n} + 2B_m\dot{\zeta}_{i2nm}, \tag{84}$$

$$\frac{\partial}{\partial B_m}\left(\frac{\partial \dot{\zeta}_i}{\partial B_n}\right) = \frac{\partial}{\partial B_m}(\dot{\zeta}_{i1n} + 2B_m\dot{\zeta}_{i2nm}) = 2\dot{\zeta}_{i2nm}, \tag{85}$$

$$\frac{\partial}{\partial \dot{\zeta}_0}(|\dot{\zeta}_0|) = \frac{|\dot{\zeta}_0|}{\dot{\zeta}_0}, \quad \frac{\partial}{\partial \dot{\zeta}_0}(|\dot{\zeta}_0|\dot{\zeta}_0) = 2|\dot{\zeta}_0|, \quad \frac{\partial}{\partial \dot{\zeta}_0}\left(\frac{|\dot{\zeta}_0|}{\dot{\zeta}_0}\right) = 0, \tag{86}$$

$$\begin{aligned}\zeta_i^2 &= (\zeta_{i0} + B_n\zeta_{i1n} + B_nB_m\zeta_{i2nm})^2 \\ &= \zeta_{i0}^2 + 2\zeta_{i0}B_n\zeta_{i1n} + B_nB_m\zeta_{i1n}\zeta_{i1m} + 2\zeta_{i0}B_nB_m\zeta_{i2nm} + \cdots,\end{aligned} \tag{87}$$

$$\begin{aligned}\zeta_i^3 &= (\zeta_{i0} + B_n\zeta_{i1n} + B_nB_m\zeta_{i2nm})^3 \\ &= \zeta_{i0}^3 + 3\zeta_{i0}^2B_n\zeta_{i1n} + 3\zeta_{i0}B_nB_m\zeta_{i1n}\zeta_{i1m} + 3\zeta_{i0}^2B_nB_m\zeta_{i2nm} + \cdots.\end{aligned} \tag{88}$$

B.2. Taylor's series expansion

Taylor's series expansion of $|\dot{\zeta}_0|\dot{\zeta}_0$ appearing in Eq. (35) about $B_n = B_m = 0$ ($B_n = 0$ and $B_n = B_m = 0$ are indicated with the subscript 0)

$$|\dot{\zeta}_0|\dot{\zeta}_0 = |\dot{\zeta}_{00}|\dot{\zeta}_{00} + B_n\left.\frac{\partial|\dot{\zeta}_0|\dot{\zeta}_0}{\partial B_n}\right|_0 + \frac{1}{2}B_nB_m\left.\frac{\partial^2|\dot{\zeta}_0|\dot{\zeta}_0}{\partial B_n\,\partial B_m}\right|_0, \tag{89}$$

where

$$\left.\frac{\partial|\dot{\zeta}_0|\dot{\zeta}_0}{\partial B_n}\right|_0 = \left.\frac{\partial|\dot{\zeta}_0|\dot{\zeta}_0}{\partial\dot{\zeta}_0}\frac{\partial\dot{\zeta}_0}{\partial B_n}\right|_0 = 2|\dot{\zeta}_0|(\dot{\zeta}_{01n} + 2B_m\dot{\zeta}_{02nm})\big|_0 = 2|\dot{\zeta}_{00}|\dot{\zeta}_{01n} \tag{90}$$

and

$$\left.\frac{\partial^2|\dot{\zeta}_0|\dot{\zeta}_0}{\partial B_n \partial B_m}\right|_0 = \frac{\partial}{\partial B_m}\left.\left(\frac{\partial|\dot{\zeta}_0|\dot{\zeta}_0}{\partial \dot{\zeta}_0}\frac{\partial \dot{\zeta}_0}{\partial B_n}\right)\right|_0 = 2\frac{\partial}{\partial B_m}\left.\left(|\dot{\zeta}_0|\frac{\partial \dot{\zeta}_0}{\partial B_n}\right)\right|_0$$
$$= 2\left.\left[\frac{\partial|\dot{\zeta}_0|}{\partial \dot{\zeta}_0}\frac{\partial \dot{\zeta}_0}{\partial B_m}\frac{\partial \dot{\zeta}_0}{\partial B_n} + |\dot{\zeta}_0|\frac{\partial}{\partial B_m}\left(\frac{\partial \dot{\zeta}_0}{\partial B_n}\right)\right]\right|_0 = 2\left(\frac{|\dot{\zeta}_{00}|}{\dot{\zeta}_{00}}\dot{\zeta}_{01n}\dot{\zeta}_{01m} + 2|\dot{\zeta}_{00}|\dot{\zeta}_{02nm}\right), \tag{91}$$

therefore Eq. (89) can be written as follows:

$$|\dot{\zeta}_0|\dot{\zeta}_0 = |\dot{\zeta}_{00}|\left[\dot{\zeta}_{00} + 2B_n\dot{\zeta}_{01n} + B_nB_m\left(\frac{1}{\dot{\zeta}_{00}}\dot{\zeta}_{01n}\dot{\zeta}_{01m} + 2\dot{\zeta}_{02nm}\right)\right]. \tag{92}$$

Taylor's series expansion of $|\dot{\zeta}_0|\dot{\zeta}_1$ about $B_n = B_m = 0$:

$$|\dot{\zeta}_0|\dot{\zeta}_1 = |\dot{\zeta}_{00}|\dot{\zeta}_{01} + B_n\left.\frac{\partial|\dot{\zeta}_0|\dot{\zeta}_1}{\partial B_n}\right|_0 + \frac{1}{2}B_nB_m\left.\frac{\partial^2|\dot{\zeta}_0|\dot{\zeta}_1}{\partial B_n\,\partial B_m}\right|_0, \tag{93}$$

where

$$\left.\frac{\partial|\dot{\zeta}_0|\dot{\zeta}_1}{\partial B_n}\right|_0 = \left.\frac{\partial|\dot{\zeta}_0|}{\partial B_n}\dot{\zeta}_1\right|_0 + |\dot{\zeta}_0|\left.\frac{\partial \dot{\zeta}_1}{\partial B_n}\right|_0 = \left.\frac{\partial|\dot{\zeta}_0|}{\partial \dot{\zeta}_0}\frac{\partial \dot{\zeta}_0}{\partial B_n}\dot{\zeta}_1\right|_0 + |\dot{\zeta}_0|\left.\frac{\partial \dot{\zeta}_1}{\partial \dot{\zeta}_1}\frac{\partial \dot{\zeta}_1}{\partial B_n}\right|_0$$
$$= \left.\frac{|\dot{\zeta}_0|}{\dot{\zeta}_0}(\dot{\zeta}_{01n} + 2B_m\dot{\zeta}_{02nm})(\dot{\zeta}_{10} + B_n\dot{\zeta}_{11n} + B_nB_m\dot{\zeta}_{12nm})\right|_0$$
$$+ |\dot{\zeta}_0|(\dot{\zeta}_{11n} + 2B_m\dot{\zeta}_{12nm})\big|_0 = |\dot{\zeta}_{00}|\left(\frac{\dot{\zeta}_{10}}{\dot{\zeta}_{00}}\dot{\zeta}_{01n} + \dot{\zeta}_{11n}\right) \tag{94}$$

and

$$\left.\frac{\partial^2|\dot{\zeta}_0|\dot{\zeta}_1}{\partial B_n\,\partial B_m}\right|_0 = \frac{\partial}{\partial B_m}\left.\left(\frac{|\dot{\zeta}_0|}{\dot{\zeta}_0}\frac{\partial \dot{\zeta}_0}{\partial B_n}\dot{\zeta}_1 + |\dot{\zeta}_0|\frac{\partial \dot{\zeta}_1}{\partial B_n}\right)\right|_0$$
$$= \frac{\partial}{\partial \dot{\zeta}_0}\left(\frac{|\dot{\zeta}_0|}{\dot{\zeta}_0}\right)\frac{\partial \dot{\zeta}_0}{\partial B_m}\frac{\partial \dot{\zeta}_0}{\partial B_n}\dot{\zeta}_1 + \frac{|\dot{\zeta}_0|}{\dot{\zeta}_0}\frac{\partial^2 \dot{\zeta}_0}{\partial B_m\,\partial B_n}\dot{\zeta}_1 + \left.\frac{|\dot{\zeta}_0|}{\dot{\zeta}_0}\frac{\partial \dot{\zeta}_0}{\partial B_n}\frac{\partial \dot{\zeta}_1}{\partial B_m}\right|_0$$
$$+ \frac{\partial|\dot{\zeta}_0|}{\partial \dot{\zeta}_0}\frac{\partial \dot{\zeta}_0}{\partial B_m}\frac{\partial \dot{\zeta}_1}{\partial B_n} + |\dot{\zeta}_0|\left.\frac{\partial^2 \dot{\zeta}_1}{\partial B_m\,\partial B_n}\right|_0$$
$$= 2\frac{|\dot{\zeta}_0|}{\dot{\zeta}_0}\dot{\zeta}_{02nm}\dot{\zeta}_1 + \left.\frac{|\dot{\zeta}_0|}{\dot{\zeta}_0}(\dot{\zeta}_{01n} + 2B_m\dot{\zeta}_{02nm})(\dot{\zeta}_{11m} + 2B_n\dot{\zeta}_{12nm})\right|_0$$
$$+ \left.\frac{|\dot{\zeta}_0|}{\dot{\zeta}_0}(\dot{\zeta}_{01m} + 2B_n\dot{\zeta}_{02nm})(\dot{\zeta}_{11n} + 2B_m\dot{\zeta}_{12nm}) + 2|\dot{\zeta}_0|\dot{\zeta}_{12nm}\right|_0$$
$$= |\dot{\zeta}_{00}|\left(2\frac{\dot{\zeta}_{10}}{\dot{\zeta}_{00}}\dot{\zeta}_{02nm} + \frac{1}{\dot{\zeta}_{00}}\dot{\zeta}_{01n}\dot{\zeta}_{11m} + \frac{1}{\dot{\zeta}_{00}}\dot{\zeta}_{01m}\dot{\zeta}_{11n} + 2\dot{\zeta}_{12nm}\right) \tag{95}$$

therefore Eq. (93) can be written as follows:

$$|\dot{\zeta}_0|\dot{\zeta}_1 = |\dot{\zeta}_{00}|\left[\dot{\zeta}_{01} + B_n\left(\frac{\dot{\zeta}_{10}}{\dot{\zeta}_{00}}\dot{\zeta}_{01n} + \dot{\zeta}_{11n}\right)\right.$$
$$\left. + \frac{1}{2}B_nB_m\left(2\frac{\dot{\zeta}_{10}}{\dot{\zeta}_{00}}\dot{\zeta}_{02nm} + \frac{1}{\dot{\zeta}_{00}}\dot{\zeta}_{01n}\dot{\zeta}_{11m} + \frac{1}{\dot{\zeta}_{00}}\dot{\zeta}_{11n}\dot{\zeta}_{01m} + 2\dot{\zeta}_{12nm}\right)\right]. \tag{96}$$

B.3. Mathematics developments of Eq. (35)

By considering Eq. (36), left-hand terms of (35) can be written as follows:

$$\begin{aligned}&\ddot{\zeta}_i + a_1\dot{\zeta}_i + a_2\zeta_i + 3a_4\xi^2\zeta_i\\&\quad= \ddot{\zeta}_{i0} + B_n\ddot{\zeta}_{i1n} + B_nB_m\ddot{\zeta}_{i2nm} + a_1(\dot{\zeta}_{i0} + B_n\dot{\zeta}_{i1n} + B_nB_m\dot{\zeta}_{i2nm})\\&\qquad + a_2(\zeta_{i0} + B_n\zeta_{i1n} + B_nB_m\zeta_{i2nm}) + 3a_4B_nB_m\chi_n\chi_m(\zeta_{i0} + B_n\zeta_{i1n} + B_nB_m\zeta_{i2nm})\end{aligned} \tag{97}$$

by ordering Eq. (97) the following set of relationships can be written:

$$\begin{cases}\ddot{\zeta}_{i0} + a_1\dot{\zeta}_{i0} + a_2\zeta_{i0}\\ \ddot{\zeta}_{i1n} + a_1\dot{\zeta}_{i1n} + a_2\zeta_{i1n}\\ \ddot{\zeta}_{i2nm} + a_1\dot{\zeta}_{i2nm} + a_2\zeta_{i2nm} + 3a_4\chi_n\chi_m\zeta_{i0}.\end{cases} \tag{98}$$

By remembering Eq. (21), right-hand terms of (35) can be written as follows.
First equation:

$$(1-a_5)\ddot{\xi} + a_1\dot{\xi} + a_4\xi^3 + a_2\xi = (1-a_5)B_n\ddot{\chi}_n + a_1B_n\dot{\chi}_n + a_4B_nB_mB_l\chi_n\chi_m\chi_l + a_2B_n\chi_n \tag{99}$$

and by ordering:

$$\begin{cases}0\\ (1-a_5)\ddot{\chi}_n + a_1\dot{\chi}_n + a_2\chi_n\\ 0.\end{cases} \tag{100}$$

Second equation:

$$\begin{aligned}&3a_4\xi\zeta_0^2 - a_3|\dot{\zeta}_0|\dot{\zeta}_0 - a_4\zeta_0^3\\&\quad= 3a_4B_n\chi_n(\zeta_{00} + B_n\zeta_{01n} + B_nB_m\zeta_{02nm})\\&\qquad - a_3|\dot{\zeta}_{00}|\left[\dot{\zeta}_{00} + 2B_n\dot{\zeta}_{01n} + B_nB_m\left(\frac{1}{\dot{\zeta}_{00}}\dot{\zeta}_{01n}\dot{\zeta}_{01m} + 2\dot{\zeta}_{02nm}\right)\right]\\&\qquad - a_4(\dot{\zeta}_{00}^3 + 3\dot{\zeta}_{00}^2B_n\dot{\zeta}_{01n} + 3\dot{\zeta}_{00}B_nB_m\dot{\zeta}_{01n}\dot{\zeta}_{01m} + 3\dot{\zeta}_{00}^2B_nB_m\dot{\zeta}_{02nm})\end{aligned} \tag{101}$$

and by ordering:

$$\begin{cases}-a_3|\dot{\zeta}_{00}|\dot{\zeta}_{00} - a_4\dot{\zeta}_{00}^3\\ -2a_3|\dot{\zeta}_{00}|\dot{\zeta}_{01n} - 3a_4(\dot{\zeta}_{00}^2\dot{\zeta}_{01n} + \zeta_{00}\chi_n)\\ 3a_4[\zeta_{01n}\chi_m - \dot{\zeta}_{00}(\dot{\zeta}_{01n}\dot{\zeta}_{01m} + \dot{\zeta}_{00}\dot{\zeta}_{02nm})] - a_3|\dot{\zeta}_{00}|\left(\frac{1}{\dot{\zeta}_{00}}\dot{\zeta}_{01n}\dot{\zeta}_{01m} + 2\dot{\zeta}_{02nm}\right).\end{cases} \tag{102}$$

Third equation:

$$\begin{aligned}&6a_4\xi^2\zeta_0\zeta_1 - 2a_3|\dot{\zeta}_0|\dot{\zeta}_1 - 3a_4\zeta_0^2\zeta_1\\&\quad= 6a_4B_n\chi_n(\zeta_{00} + B_n\zeta_{01n} + B_nB_m\zeta_{02nm})(\zeta_{10} + B_n\zeta_{11n} + B_nB_m\zeta_{12nm})\\&\qquad - 2a_3|\dot{\zeta}_{00}|\left[\dot{\zeta}_{01} + B_n\left(\frac{\dot{\zeta}_{10}}{\dot{\zeta}_{00}}\dot{\zeta}_{01n} + \dot{\zeta}_{11n}\right)\right.\\&\qquad \left. + \frac{1}{2}B_nB_m\left(2\frac{\dot{\zeta}_{10}}{\dot{\zeta}_{00}}\dot{\zeta}_{02nm} + \frac{1}{\dot{\zeta}_{00}}\dot{\zeta}_{01n}\dot{\zeta}_{11m} + \frac{1}{\dot{\zeta}_{00}}\dot{\zeta}_{11n}\dot{\zeta}_{01m} + 2\dot{\zeta}_{12nm}\right)\right]\\&\qquad - 3a_4(\zeta_{00}^2 + 2\zeta_{00}B_n\zeta_{01n} + B_nB_m\zeta_{01n}\zeta_{i1m}\\&\qquad + 2\zeta_{00}B_nB_m\zeta_{02nm})(\zeta_{10} + B_n\zeta_{11n} + B_nB_m\zeta_{12nm})\end{aligned} \tag{103}$$

and by ordering:

$$\begin{cases} -2a_3|\dot{\zeta}_{00}|\dot{\zeta}_{01} - 3a_4\zeta_{00}^2\zeta_{10} \\ -2a_3|\dot{\zeta}_{00}|\left(\frac{\dot{\zeta}_{10}}{\dot{\zeta}_{00}}\dot{\zeta}_{01n} + \dot{\zeta}_{11n}\right) - 3a_4(\zeta_{00}^2\zeta_{11n} + 2\zeta_{00}\zeta_{10}\zeta_{01n} + 2\zeta_{00}\zeta_{10}\chi_n) \\ -a_3|\dot{\zeta}_{00}|\left(2\frac{\dot{\zeta}_{10}}{\dot{\zeta}_{00}}\dot{\zeta}_{02nm} + \frac{1}{\dot{\zeta}_{00}}\dot{\zeta}_{01n}\dot{\zeta}_{11m} + \frac{1}{\dot{\zeta}_{00}}\dot{\zeta}_{11n}\dot{\zeta}_{01m} + 2\dot{\zeta}_{12nm}\right) \\ -3a_4[\zeta_{00}^2\zeta_{12nm} + \zeta_{10}\zeta_{01n}\zeta_{01m} + 2\zeta_{00}\zeta_{01n}\zeta_{11n} - 2\chi_n(\zeta_{00}\zeta_{11n} + \zeta_{01n}\zeta_{10})]. \end{cases} \tag{104}$$

References

[1] L.V.S. Sagrilo, M.Q. Siqueira, G.B. Ellwanger, E.C.P. Lima, M.D.A.S. Ferreira, M.M. Mourelle, A coupled approach for dynamic analysis of CALM systems, *Applied Ocean Research* 24 (1) (2002).

[2] R. Ruinen, G. Dagencamp, Anchoring of floating production systems, *Journal of Offshore Technology* 11 (1) (2003).

[3] M.B. Rosales, C.P. Filipich., Full modeling of the mooring non-linearity in a two-dimensional floating structure, *International Journal of Non-Linear Mechanics* 41 (1) (2006).

[4] O.C. Zienkiewicz, R.W. Lewis, K.G. Stagg, *Numerical Methods in Offshore Engineering*, Wiley, New York, 1978.

[5] H.M. Irvine, *Cable Structures*, The MIT Press, Cambridge, MA, 1981.

[6] O.M. Faltinsen, *Sea Loads on Ships and Off-shore Structures*, Cambridge University Press, Cambridge, 1990.

[7] N. Newman, *Marine Hydrodynamics*, The MIT Press, Cambridge, MA, 1977.

[8] A. Culla, A. Carcaterra, Statistical linearization of cable equations: an application to a guyed tower offshore structure, *Proceedings of the Second International Conference on Hydroelaticity in Marine Tecnology*, 1–3 December 1998, Fukuoka (Japan).

[9] A. Culla, A. Carcaterra, Modelli di cavi sommersi tridimensionali a parametri concentrati sottoposti a forze stocastiche (in Italian), *16th AIMETA Congress of Theoretical and Applied Mechanics*, 2003.

[10] E.S. Venstel, *Teoria della probabilità*, MIR, Moscow, 1983 (in Italian).

[11] M.K. Ochi, *Applied Probability and Stochastic Processes*, Wiley, New York, 1990.

[12] J.B. Roberts, P.D. Spanos, *Random Vibration and Statistical Linearization*, Wiley, New York, 1990.

[13] M. Jardak, C.H. Su, G.E. Karniadakis, Spectral polynomial chaos solutions of the stochastic advection equation, *Journal of Scientific Computing* 17 (1) (2002).

[14] D. Xiu, D. Lucor, C.H. Su, G.E. Karniadakis, Stochastic modelling of flow–structure interactions using generalized polynomial chaos, *Journal of Fluids Engineering—Transaction of ASME* 124 (1) (2002).

[15] D.C. Poirel, S.J. Price, Post-instability behaviour of structurally nonlinear airfoil in longitudinal turbulence, *Journal of Aircraft* 34 (5) (1997).

[16] D.C. Poirel, S.J. Price, Structurally nonlinear fluttering airfoil in turbulent flow, *AIAA Journal* 39 (10) (2001).

[17] A. Carcaterra, D. Dessi, F. Mastroddi, Hydrofoil vibration induced by a random flow: a stochastic perturbation approach, *Journal of Sound and Vibration* 283 (1–2) (2005).

[18] F. Kozin, The method of statistical linearization for non-linear stochastic vibrations, in: F. Ziegler, G.I. Schuller (Eds.), *Nonlinear Stochastic Dynamic Engineering Systems*, Springer, Berlin, 1987.

[19] L. Socha, Linearization in analysis of nonlinear stochastic systems: recent results—Part I: theory, *Applied Mechanics Reviews* 58 (2005).

[20] P. Bernard, L. Wu, Stochastic linearization: the theory, *Journal of Applied Probability* 35 (3) (1998).

[21] P. Bernard, Stochastic linearization: what is available and what is not, *Computer & Structures* 67 (1998).